

Macromolecular Nanotechnology

Tribological behavior of polyurethane-based composite coating reinforced with TiO₂ nanotubesHao-Jie Song^{a,b}, Zhao-Zhu Zhang^{a,*}, Xue-Hu Men^{a,b}^a State Key Laboratory of Solid Lubrication, Lanzhou Institute of Chemical Physics, Chinese Academy of Sciences, Lanzhou 730000, PR China^b Graduate School, Chinese Academy of Sciences, Beijing 100039, PR ChinaReceived 11 July 2007; received in revised form 15 January 2008; accepted 1 February 2008
Available online 9 February 2008

Abstract

The unmodified and hexamethylene diisocyanate (HDI) modified TiO₂ nanotubes, were used for fabricating TiO₂ nanotubes (TiNTs)/polyurethane (PU) composite coating. The effects of applied load and sliding speed on the tribological behavior of the composite coating were investigated using a block-on-ring wear tester. Compared to the TiO₂ nanotubes filled PU composite coating, the HDI modified TiO₂ nanotubes (TiNTs–HDI) filled one had the lower friction coefficient and higher wear life under various applied loads and sliding speed. Scanning electron microscope (SEM) investigation showed that the TiNTs–HDI filled PU coating had smooth worn surface under given applied load and sliding speed, and a continuous and uniform transfer film formed on the surface of the counterpart ring, which helped to reduce the wear of the coating. The improvement in the tribological properties of TiNTs–HDI/PU composite coating might due to an improvement in interfacial adhesion between TiNTs and PU after HDI treatment. The strong interfacial coupling of the composite coating made TiNTs–HDI not easy to detach from the PU matrix, and prevented the rubbing-off of PU composite coating, accordingly improved the friction and wear properties of the composite coating.

© 2008 Elsevier Ltd. All rights reserved.

Keywords: TiO₂ nanotubes; Polyurethane coating; Tribological behavior; Transfer films

1. Introduction

The US Army utilizes polyurethane coatings as camouflage ‘top-coats’ on all Army tactical vehicles and aircraft. These coatings not only serve to camouflage vehicles but also provide protection against chemical warfare agents [1]. However, if the coating requires higher loads and small clearance over the entire lifetime, Common coating

materials are less suitable because of their lower mechanical strength. The solution for these applications is the production of compounds especially reinforced with different materials and additives.

Much of the current interest in nanotubular materials was initiated by the discovery of carbon nanotubes, which are promising for many applications, particularly in the field of electronic materials. Although noncarbon nanotubes were identified in the early 1990s, relatively little research has been carried out on their synthesis and characterization. Other nanotubular materials represent a diverse

* Corresponding author. Fax: +86 931 4968098.E-mail address: zzzhang@licp.ac.cn (Z.-Z. Zhang).

chemistry, significantly extend the area of possible applications, possess unique combinations of physicochemical properties, and are often easier to synthesize than carbon nanotubes. These properties and relatively low synthesis costs can render noncarbon nanomaterials attractive for technological applications [2].

TiO₂, which is the most common compound of titanium, is often used in many applications ranging from anticorrosion, self-cleaning coatings, and paints to solar cells and photocatalysts [3–6]. Recently, much effort has been directed at obtaining TiO₂ nanotubes with a large surface area and high photocatalytic activity [7–10]. However, the friction and wear behavior of the TiO₂ nanotube filled polymer composites has not previously been performed. By reinforcing polyurethane with TiO₂ nanotubes, it might be feasible to develop high performance polyurethane-based composite coating applicable under friction and wear conditions.

With the aim of improving the dispersion of TiO₂ nanotubes and the interfacial adhesion between TiO₂ nanotubes and the polyurethane matrix, we design a scheme in which TiO₂ nanotubes first react with hexamethylene diisocyanate (HDI). HDI is selected because the active hydrogen atoms of amide of the polyurethane (PU) matrix might react with isocyanate functional groups (O=C=N—) during curing and form three-dimensional networks throughout the composite coating, so that the TiO₂ nanotubes could be connected with the PU matrix covalently and take effect desirably.

The objective of the present investigation is to study the tribological characteristics of random oriented TiO₂ nanotubes reinforced polyurethane composite coating under various experimental conditions.

2. Experiments

2.1. Materials

Single-component polyurethane (PU) was provided by Xinhua Resin Company of Shanghai, and the ash content and the isocyanate (O=C=N—)

content were 50 and 5–8 wt.%, respectively. Commercial polyfluoropolymer wax powder (Mircopowder Company, USA) which have excellent chemical resistance to acids, bases and solvents and have release and non-stick properties with an average particle size ranging from 3 to 4 μm was selected as the solid lubricant. DB-551 (γ-aminopropyl trimethoxysilane) was commercially provided by the Diamond New Material of Chemical Inc., China. Hexamethylene diisocyanate (HDI) was provided by Fluka. Dibutyltin dilaurate was supplied by Tianjin No.1 Chemical Reagent Factory, China. The mixture of acetone/xylene/cyclohexanone in a volume fraction of 4:2:1 was employed in the present work as a solvent.

In our work, steel 45 (12.7 mm × 12.7 mm × 19 mm) was used as substrate of the coating. An AISI-C-52100 ring of 49.2 mm in diameter and 12 mm in thickness (Hardness Hv850) was made of bearing steel. The chemical compositions of steel 45 and AISI-C-52100 bearing steel are shown in Table 1.

2.2. Synthesis of TiO₂ nanotubes

Experimental details were as follows: commercial TiO₂ powders (HR₃; crystalline rutile with surface area of 210 m²/g, average diameter ≤ 20 nm) were used as the TiO₂ nanotubes precursors. The TiO₂ nanotubes were synthesized with the method similar to that of Kasuga et al. [11]. The details of the preparation procedures are as follows: 0.5 g of the precursor was mixed with 40 ml of NaOH aqueous solution with the concentration of 10 mol/l, followed by hydrothermal treatment at 130 °C in a Teflon-lined autoclave for 15 h. The treated powders were washed thoroughly with water and 0.1 mol/l HCl aqueous solution until the pH value of the washing solution lower than 7.0, and finally, the white product was annealed at 400 °C for 2 h in air.

2.3. Surface treatment of TiO₂ nanotubes

The TiO₂ nanotubes were preheated at 120 °C in vacuum for 24 h to eliminate possibly absorbed

Table 1
The chemical composition of the AISI-C-52100 bearing steel and steel 45 (in wt.%)

	C	Si	Mn	P	S	Cr	Ni	Cu	Fe
Steel 45	0.42–0.5	0.17–0.37	0.50–0.80	0.035	0.035	0.25	0.25	0.25	Balance
Bear steel	0.98–1.1	0.15–0.35	0.25–0.45			1.3–1.6			Balance

water on the surface of the particles. Then, 0.5 g of TiO₂ nanotubes was added into a three-neck flask with 50.0 ml toluene and dispersed through ultrasonication (in a water bath) for 30 min. Then 10 ml of 1.0 wt.% toluene solution of DB-551 was added and stirred for 6 h at 60–65 °C for silanization. After the reaction, the DB-551 treated TiO₂ nanotubes were obtained by filtration of the solution and washing with toluene, absolute ethanol and acetone, and then drying in a vacuum oven at 80 °C overnight.

The complete scheme for the TiO₂ nanotubes modified with hexamethylene diisocyanate (HDI) can be illustrated in Fig. 1. The typical treatment of TiO₂ nanotubes proceeded as follows. A 150 ml round-bottomed flask was charged with 0.5 g of the DB-551 treated TiO₂ nanotubes, 50 ml benzene, 20 ml HDI and 2–3 drops dibutyltin dilaurate. The mixture was stirred at 80 °C for 10 h under a slow stream of N₂. The solid was separated by filtration through a 0.2-μm Millipore PVDF membrane, thoroughly washed with benzene and dried at 60 °C for 24 h under vacuum to obtain TiO₂ nanotubes modified with HDI (TiNTs–HDI).

2.4. Coating preparation

The unmodified and HDI modified TiNTs, were used to reinforce the polyurethane coating. Before the fabrication of composite coating, the two type TiNTs were sonicated the aggregation and to sus-

pend the TiNTs in solution. The polyurethane resin and the solid lubricant of polyfluo150 wax (PFW) powder were added to the solution for forming the TiNTs/polyurethane composite slurry. The quantity of PFW used was 30% of the binder of the polyurethane mass. The coatings on the steel substrates that were rinsed with acetone and roughened by spraying corundum were prepared by spraying the prepared mixture with 0.2 MPa nitrogen gas using spray gun. All the samples were cured in a container with relative humidity of 50–60% and temperature of 25 °C. After solvent evaporation, a thin coating was obtained on the substrate and then cured at 60 °C, 120 °C for 2 h, respectively. The thickness of the cured coatings was 30–50 μm.

2.5. Evaluation of the tribological behavior

An MHK-500 ring-on-block wear tester (made by the Jinan Testing Machine Factory, China) with a similar configuration to a Timken tester was used to evaluate the friction and wear behavior of the PU composite coating. The contact schematic of the frictional couple is shown in Fig. 2. A steel ring was rotated against the PU coating at speeds of 1.28–3.84 m/s and load of 320–1620 N. The sliding time of 60 min was used in all friction tests. Before each test, the steel ring was abraded with 900 grade water proof abrasive paper. Then the steel ring was cleaned with acetone followed by drying. The sliding distance was calculated from the product of

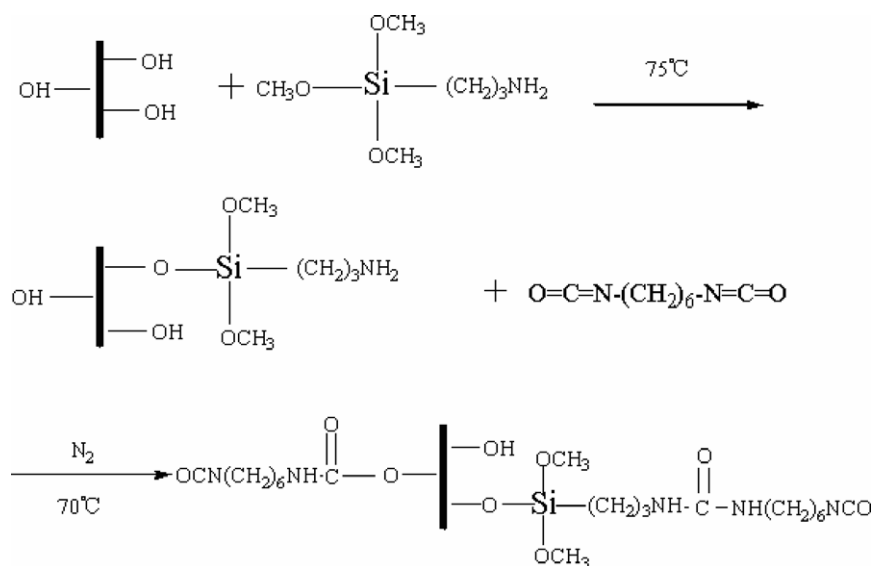


Fig. 1. The complete scheme for the TiNTs modified with hexamethylene diisocyanate (HDI).

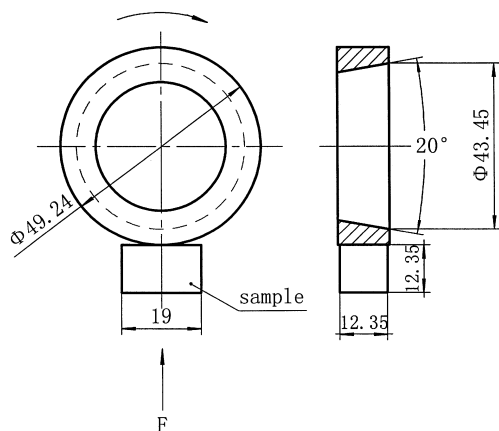


Fig. 2. Contact schematic for the frictional couple.

the sliding speed and the sliding time. The wear life of the coatings was calculated after dividing the sliding distance by the corresponding coating thickness in micrometers. All the friction and wear tests were carried out at 20–25 °C and a relative humidity of 40–60%.

3. Results and discussion

3.1. Morphology and structure of TiNTs

Fig. 3 shows SEM images of the TiNTs after hydrothermal treatment for 15 h in a 5 M NaOH solution at 150 °C, the middle width of the obtained TiNTs is 20 nm and the length is 2 μm. It was found that non-capped TiNTs tended to agglomerate and did not permit identification of a single tube owing to the high surface energy of nanotubes (Fig. 3a). After HDI modified TiNTs, The HDI-modified TiNTs in Fig. 3b show much better dispersibility.

It demonstrates that after the surfaces of TiNTs were modified by HDI, the aggregation of TiNTs was greatly reduced.

The corresponding X-ray diffraction patterns recorded from the as prepared nanotubes are shown in Fig. 4. The crystal of the nanotubes is very fine. All the relatively sharp peaks could be indexed as anatase TiO_2 with crystalline cell constants of $a = 3.785$ and $c = 9.513$ Å, which are basically in agreement with the reported values Joint Committee on Powder Diffraction Standards (JCPDS) Card No. 21–1272. There are no characteristic peaks of impurities, such as sodium titanium oxide, indicating that complete ionic exchange from Na^+ to H^+ is achieved.

3.2. FTIR analysis

Fig. 5 shows the FTIR results of the TiNTs obtained at different processing steps. The FTIR spectrum (Fig. 5a) of the unmodified TiNTs shows the two bands appeared at 3430 and 500–780 cm^{-1} , which is attributed to the —OH and Ti—O stretching vibrations, respectively. The absorption at 1060 cm^{-1} reflects Si—O—Si structure that is produced by hydrolysis and polycondensation of the coupling agent (Fig. 5b). The absorption peaks near 2900 cm^{-1} , 1455 cm^{-1} and 1400 cm^{-1} are ascribed to CH_3 — and $-(\text{CH}_2)-$ groups of the coupling agent. Because the $-\text{NH}_2$ groups were introduced on the surface of TiNTs, it is very beneficial for these functional groups to anchor HDI molecule on the surface of TiNTs through the covalent bond between the $-\text{NH}_2$ groups of TiNTs and $-\text{N}=\text{C}=\text{O}$ groups of HDI. These peaks are visibly enhanced by subsequent HDI treatment for more introduced $-(\text{CH}_2)-$ groups and their location

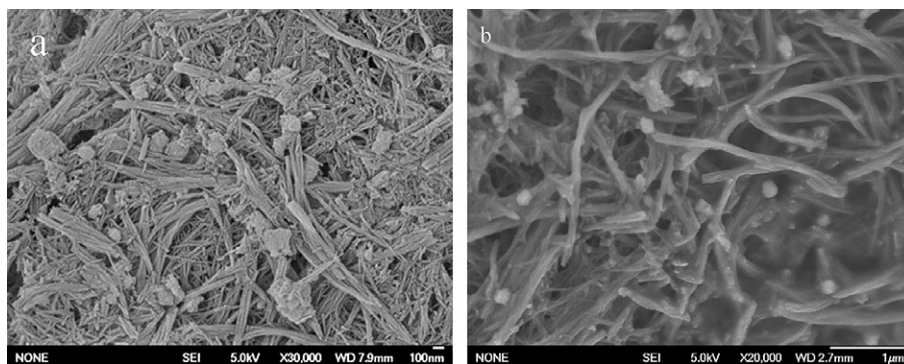


Fig. 3. The SEM micrograph of TiNTs: (a) the unmodified TiNTs; (b) HDI modified TiNTs.

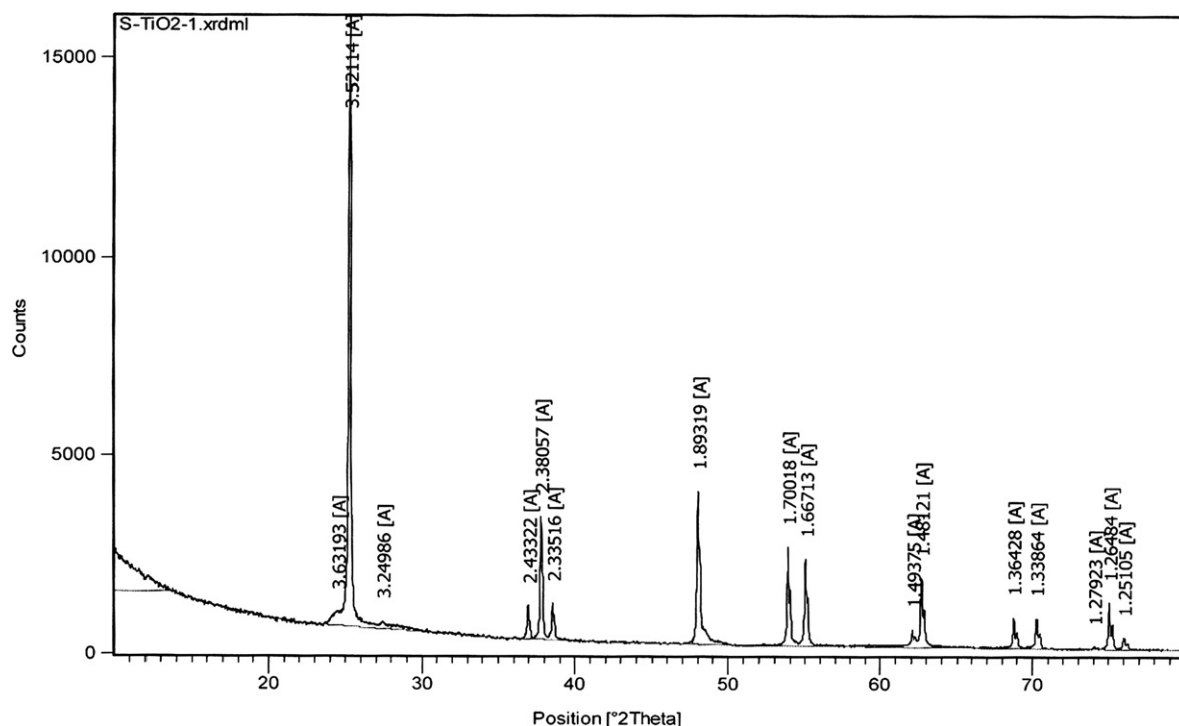


Fig. 4. XRD patterns of the prepared TiO₂ nanotubes.

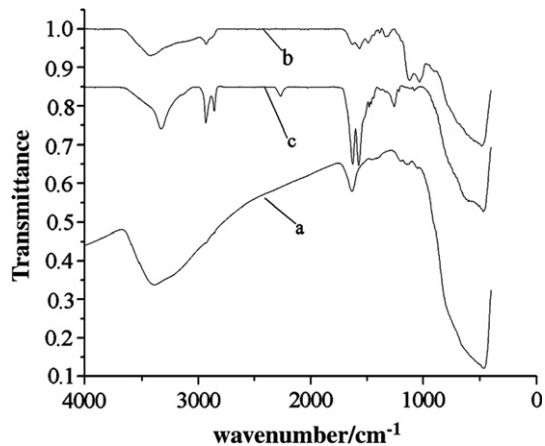


Fig. 5. The FTIR results of the TiNTs obtained at different processing steps: (a) The unmodified TiNTs; (b) the DB-551 modified TiNTs; (c) the HDI modified TiNTs.

shifted a little because of the effect of $-\text{CH}_2-\text{N}=\text{C}=\text{O}$, which comes from monomers of HDI. Significantly, the new absorption at 2273 cm^{-1} that reflects $-\text{N}=\text{C}=\text{O}$ double bond groups appear after HDI treatment. From the spectra, it can be deduced that the coupling agent DB-551 has been grafted on TiO₂ nanotubes and reacted

with monomers to produce a layer of HDI connecting with TiO₂ nanotubes via coupling agent.

3.3. Friction and wear behaviors

The steady-state friction coefficient and specific wear life of the PU composite coatings under dry sliding was shown in Table 2. It is seen that addition of 1.0 wt.% of TiNTs or TiNTs–HDI can lead to a decrease in the friction coefficient of the PU coating. The PU coating reinforced with 1.0 wt.% of TiNTs–HDI holds the lowest friction coefficient among the three composite coatings. Furthermore, we found that TiNTs–HDI as the filler were superior to TiNTs in terms of the ability to increase the wear resistance of the PU coating. The wear life of the PU coating

Table 2

The friction coefficient and wear life of composite coating under water lubrication and dry sliding (applied load of 320 N and velocity of 2.56 m/s)

Composite coating	Friction coefficient, μ	Wear life ($\text{m } \mu\text{m}^{-1}$)
PU + 30% PFW	0.175	535
PU + 30% PFW + 1.0% TiNTs	0.158	2287
PU + 30% PFW + 1.0% TiNTs–HDI	0.137	2737

filled with 1.0 wt.% of TiNTs is increased by nearly 200% as compared to that of the unfilled one. The wear life of the one filled with 1.0 wt.% of TiNTs–HDI is improved by about 250% as compared to that of the unfilled one. The friction-reduction and anti-wear ability of the modified TiNTs with HDI as lubricant additive can be explained by well dispersion and superior property of TiNTs. Because the unmodified TiNTs presented poor dispersion in PU binder, the large TiNTs bundles were easily formed in PU coating, resulting in the friction coefficient increasing. However, TiNTs were released from the TiNTs/PU composite coating during sliding and transferred to the interface between the PU composite coating and the steel counter-face. The TiNTs in the interface served as spacers, preventing the direct contact between the two mating surfaces, thereby slowing the wear rate. After modified with HDI, the TiNTs could be dispersed in PU binder uniformly. So, two mating wear surfaces were easily filled with the dispersed TiNTs during the wear process, and then the TiNTs on wear surface could serve as spacers, preventing rough contact between the two mating wear surfaces, thereby decreasing the wear loss considerably. In addition, owing to TiNTs being shortened, the short and tube shape of the TiNTs would provide very easy shear and more easily slide or roll between the two mating wear surfaces, so the friction coefficient decreased greatly.

The variations of friction coefficient and wear life with applied load are depicted in Fig. 6. It was very evident that the friction coefficient and the wear life of the filled PU composite coating all decreased with increasing applied load. It is worth to note that the

PU coating containing the modified TiNTs with HDI presented lower friction coefficient and higher wear life than the one containing TiNTs. It is known that polymers are a visco-elastic materials their deformation under load is viscoelastic. Therefore, the variation of friction coefficient with load follows the equation $\mu = KN^{n-1}$ where μ is the coefficient of friction, N is the load, k constant and n is also a constant, its value $2/3 < n < 1$ [12]. According to this equation, the friction coefficient decreases with the load increase.

It is well known that wear process involves fracture, tribochemical effects and plastic flow. Transitions between regions dominated by each of these commonly give rise to changes in wear rate with load. Furthermore, this result is closely related to structure characteristics, and chemical effects occurred in frictional processes as well as transfer film formation on the counterface.

Fig. 7 shows effect of sliding speed on the friction coefficient and the wear life of the TiNTs or TiNTs–HDI filled PU coatings under 320 N. It can be seen that the friction coefficient of the TiNTs or TiNTs–HDI filled PU coating slightly decreases with increasing sliding speed. The wear life of the two-filled PU coating slightly increases when sliding speed is below 2.56 m/s and then decreases as the sliding speed rose from 2.56 m/s to 3.84 m/s. Accordingly, it should be pointed out here that the PU coating filled with 1.0 wt.% of TiNTs–HDI presented lower friction coefficient and higher wear life than the one filled with 1.0 wt.% of TiNTs when the sliding speed is below 3.84 m/s. It could be rational to infer that the sliding surface temperature of the

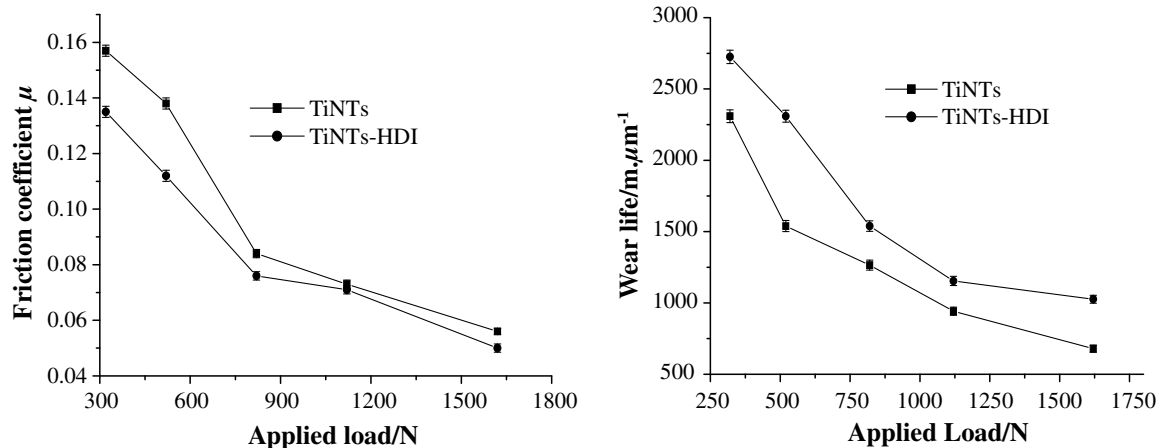


Fig. 6. Effect of applied load on the friction coefficient and the wear life of the PU coating filled with 1.0 wt.% of TiNTs or 1.0 wt.% of TiNTs–HDI under 2.56 m/s.

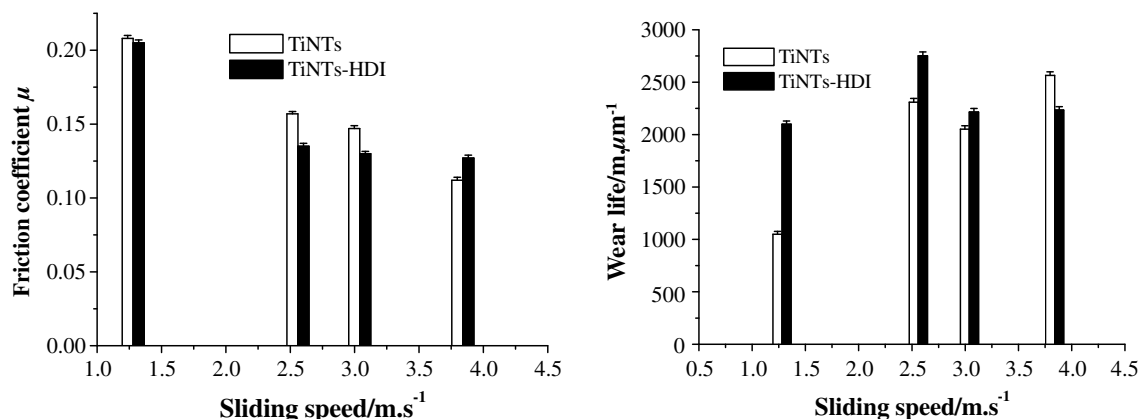


Fig. 7. Effect of sliding speed on the friction coefficient and the wear life of the PU coating filled with 1.0 wt.% of TiNTs or 1.0 wt.% of TiNTs-HDI under 320 N.

PU nanocomposite coatings increased with sliding speed, which resulted in micro-melting of the nanocomposite coating surface. Such a kind of micro-melting could be speeded at a relatively larger sliding speed, owing to the extended sliding distance. Therefore it might be rational to deduce that the formation of a transfer films of the nanocomposite coating on the counterpart steel surface was speeded as well at a relatively larger sliding speed.

Subsequently, a decreased friction coefficient and increased wear life was observed with the change from the sliding of the steel against the nanocomposite coating to that of the nanocomposite coating against its transfer film on the counterpart steel surface.

As a matter of fact, there are numerous sliding applications in which water or oil is either deliberately

introduced as a coolant, e.g. in rolling mill bearing, or present as a working fluid, e.g. in pumps. Thus, it is imperative to carry out the corresponding research on the tribological behavior of polymer composite coating at different work conditions. Fig. 8 shows the effect of immersion time in water or liquid paraffin on the tribological behavior of the 1.0 wt.% of TiNTs-HDI filled PU coating. It can be seen that the friction coefficient and the wear rate of the filled PU composite coating immersed in water all increases with increasing immersion time. However, the friction coefficient of the one immersed in liquid paraffin retains nearly unchanged when immersion time increases further, and the wear life first increases with immersion time increase and then retains unchanged when immersion time goes up further. It is worth to note that the filled PU coating immersed

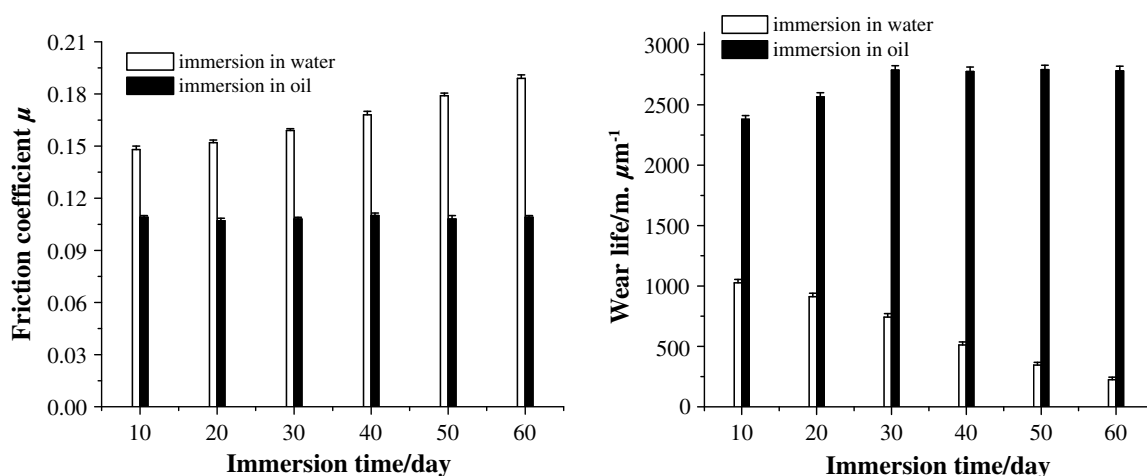


Fig. 8. Effect of immersion time in water or oil on the friction coefficient and the wear life of the PU coating filled with 1.0 wt.% of TiNTs-HDI (520 N, 2.56 m/s).

in liquid paraffin presented lower friction coefficient and higher wear life than that in water.

When the TiNTs–HDI filled PU coating immersed in water, water might be penetrated into the matrix by a two-step mechanism: first, water is absorbed by capillary action into the voids associated with interfaces between the fillers and the PU binder; then, a slow diffusion of water into the void of the bulk PU resins takes place [13,14]. The swelling of surface layers increases the shear strength of composite coating, thus, enhancing its friction coefficient. Furthermore, water absorption of polymer coating can cause loss of adhesion and blistering. Water penetration enables corrosion agents to diffuse through coating, forming electrolyte on metal surface, accompanying electrochemical dissolution. Thus, the structure of the TiNTs–HDI filled PU coating immersed in water can be greatly deteriorated, leading to the decrease of the friction and wear behavior.

Presented in Fig. 9 are the typical evolutions of the friction coefficient of 1.0 wt.% TiNTs–HDI filled PU coating as a function of the sliding time at 2.56 m/s and under different load. It can be seen that the frictional process contains the severe friction process and the smooth friction process, and the friction coefficient at the severe friction process is much higher than that at the smooth friction process. At the same time, as applied load increases, the friction coefficient of the filled PU coating is also following the reverse trend. When applied load is increased, the newly formed debris would form a more integrated but thinner films on the worn surface and as a result, the smaller debris and more integrated but thinner film on the worn surface would bring about smaller friction coefficient

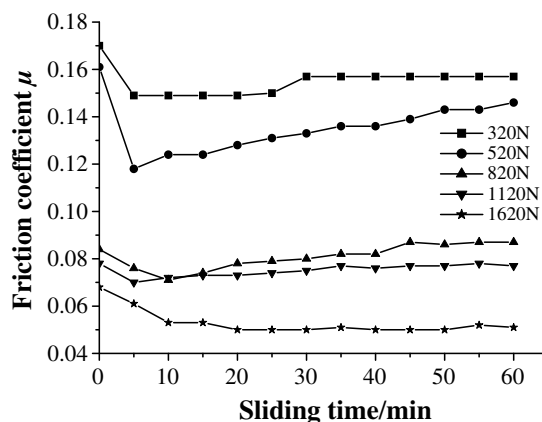


Fig. 9. Effect of sliding time on the friction coefficient of the TiNTs–HDI filled PU coating under different applied load (sliding speed: 2.56 m/s).

because of decreased degree of two-body abrasive wear [15].

3.4. TG analysis

The effect of the TiNTs–HDI on the thermal stability of the PU coating was estimated using TGA analysis. The TGA curves were obtained by heating the sample up to 780 °C at a rate of 20 °C/min with N₂ gas purging (Fig. 10). As shown in Fig. 10, the unfilled PU coating began to degrade at approximately 200 °C and was completely decomposed at 500 °C, and approximately 1.0 wt.% of the TiNTs–HDI in the PU coating began to degrade at approximately 300 °C and was completely decomposed at 600 °C. Furthermore, Fig. 10 indicates that the TiNTs–HDI filled PU composite coating decomposes at higher temperature, which suggests that the incorporation of TiNTs–HDI increases the thermal stability of the PU coating. It is well-known that the enhanced thermal conductivity of a polymer composite can facilitate heat transport and increase its thermal stability through the incorporation of high thermal conducting TiNTs–HDI.

3.5. SEM analysis

Fig. 11 shows the SEM morphologies of the worn surfaces of the unfilled and TiNTs or TiNTs–HDI filled PU coating under 320 N and 2.56 m/s, respectively. The worn surface of the unfilled PU coating shows signs of adhesion and abrasive wear (Fig. 11a). The corresponding surface is very rough, displaying plucked and ploughed marks indicative of adhesive wear and ploughing. While a close view

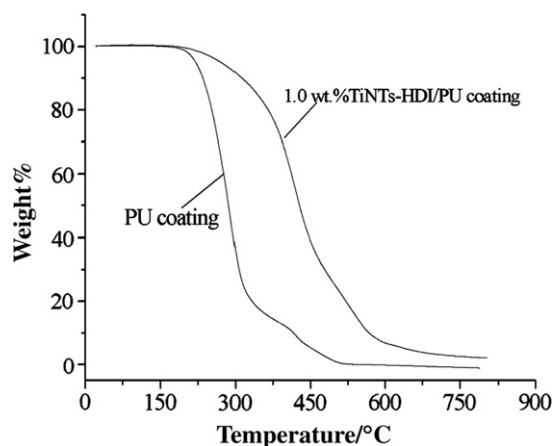


Fig. 10. TGA curves of the unfilled and 1 wt.% TiNTs–HDI filled PU composite coating.

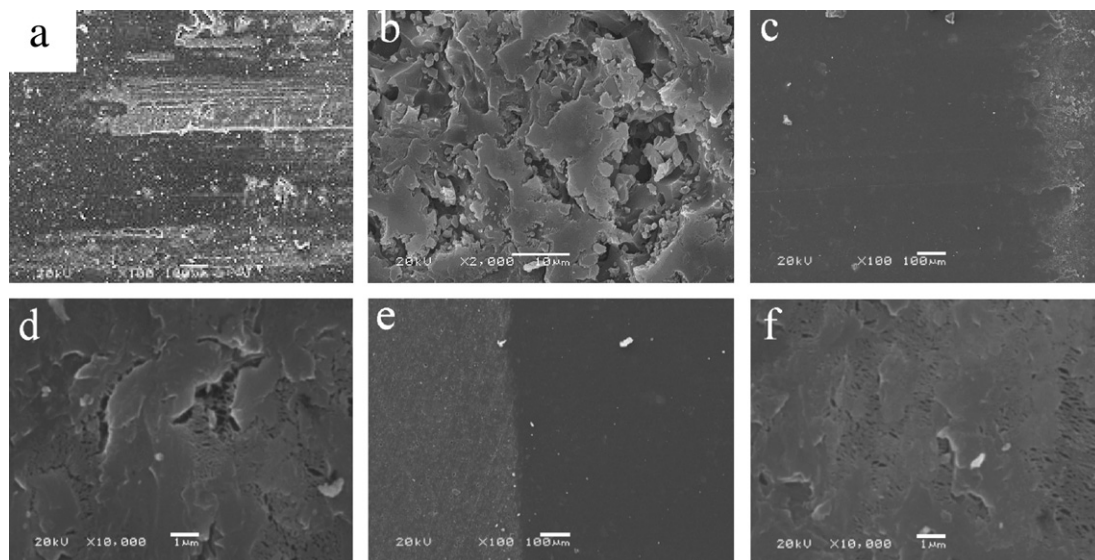


Fig. 11. SEM images of the worn surface of the unfilled and TiNTs or TiNTs–HDI filled PU coating (320 N, 2.56 m/s and 60 min): (a) the unfilled; (b) the higher magnification of (a); (c) with 1.0 wt.% of TiNTs; (d) the higher magnification of (c); (e) with 1.0 wt.% of TiNTs–HDI; (f) the higher magnification of (e).

(Fig. 11b) shows that micrometer size blocks of the PU coating materials have left the surface of the materials. This is indicative for fatigue-delamination generated under repeated loading during sliding. Fatigue wear has been regarded as a main mechanism responsible for the sliding of the unfilled PU coating against a hard counterpart [16]. The model is based on the sub-surface crack nucleation and coalescence due to shear deformation of the softer surface induced by the traction of the harder asperities [17]. This phenomenon corresponds to the relatively poorer wear resistance of the unfilled PU coating in sliding against the steel. By contrast, the scuffing and adhesion on the worn surface of the PU/1.0 wt.% TiNTs composite coating are considerably reduced (Fig. 11c). We can see a relatively smooth, uniform, and compact worn surface, which is in good agreement with the considerably increased wear resistance of the PU/TiNTs composite coating. Therefore, it can be deduced that the incorporation of TiNTs contributes to restrain the scuffing and adhesion of the PU matrix in sliding against the steel counterpart. However, close examination of the pictures at higher magnification (Fig. 11d) shows that micro-cracks in the region of the nanotube/matrix interface occurred, caused by poor dispersion in PU binder. With the propagation of these interfacial cracks, the nanotubes exposed to the asperities of the counterpart are finally removed, leaving voids on the worn surface. Moreover, it should be to note that

the worn surface of the PU/TiNTs–HDI composite coating shows a similar appearance to that of the PU/TiNTs coating, as shown in Fig. 11e. It is hard to observe wear tracks and plastic deformation and exfoliation on the worn surface. The wear scars were only observed on the protruding parts of surface, which indicated that abrasive wear and adhesive wear were not predominant. The improvement on tribological behaviors of the TiNTs–HDI filled composite coating could be attributed to the enhancement of the interfacial adhesion strength of the nanotubes and matrix after nanotube surface treatments. With a magnified view, as seen in Fig. 11f, the image of the filled PU coating identifies the presence of many individual TiNTs–HDI embedded within the PU matrix, which imply that the TiNTs–HDI were well separated in PU matrix and protected from aggregating with one another by functionalization. These phenomena must be correlated with the role of the grafted HDI. Actually, TiNTs–HDI are very difficult to be uniformly dispersed in PU binder because of the strong attraction between the TiNTs–HDI and the limited shear force during compounding. These results indicate that the PU/TiNTs–HDI composite coating exhibited higher wear resistance than the PU/TiNTs composite coating at sliding condition.

The prominent friction and wear mechanisms of PU/TiNTs or PU/TiNTs–HDI composite coating in dry sliding against a steel ring counterpart may

be attributed to the following factors: firstly, tribological results suggest that both applied stress during indentation and frictional stresses transfer to the TiNTs or TiNTs–HDI. TiNTs or TiNTs–HDI addition might contribute to increasing the local compressive and shear strength. Secondly, the incorporation of TiNTs or TiNTs–HDI in PU coating helps to considerably increase the mechanical properties of the composite coating, hence the PU/TiNTs or PU/TiNTs–HDI composite coating show much better wear resistance than the unfilled PU. Secondly, TiNTs–HDI dispersed uniformly in the composite coating can prevent the close touch of the two contact surfaces between the steel ring counter face and the composite coating, which slows the wear rate and reduces the friction coefficient. Finally, during the course of friction and wear, TiNTs are released from the PU/TiNTs composite coating and transferred to the interface between the composite coating and the steel counter face. The self-lubricate properties of TiNTs–HDI result in reduction of the wear rate and the friction coefficient.

The tribological behaviors of the filled PU coating are strongly influenced by their ability to form a transfer film on the counterface. Once a transfer film is formed, subsequent interaction occurs between polymer coating and transfer films of simi-

lar composition instead of polymer counterface. In order to further study the friction and wear mechanism of the TiNTs or TiNTs–HDI filled PU composite coating, we investigated the micrographs of the counterpart surface of three kinds of PU composite coating at 320 N and 2.56 m/s. The micrographs of the transfer films formed on the surfaces of steel rings are shown in Fig. 12. It can be seen from Fig. 12a that the transfer film of the unfilled PU coating appears to be rough and discontinuous, and is easy to scale off during friction process, so the protection from transfer film is nonexistent. In contrast, the transfer films of the TiNTs or TiNTs–HDI filled coatings (Fig. 12b and c) appear to be much smoother than that of the unfilled coating. The continuous transfer films can effectively reduce the ‘direct contact’ of the composite coating with asperities of the metallic counterpart surface. As a result, the sub-surface stresses of the composite coating can be maintained at lower values and thus lower friction coefficient and higher wear life are achieved. The results indicate that the TiNTs can strengthen the bond between the transfer film and the counterpart surface, which is able to keep the softer composite material from being damaged.

The PU coatings filled with 1.0 wt.% TiNTs–HDI are selected as an example to investigate effect

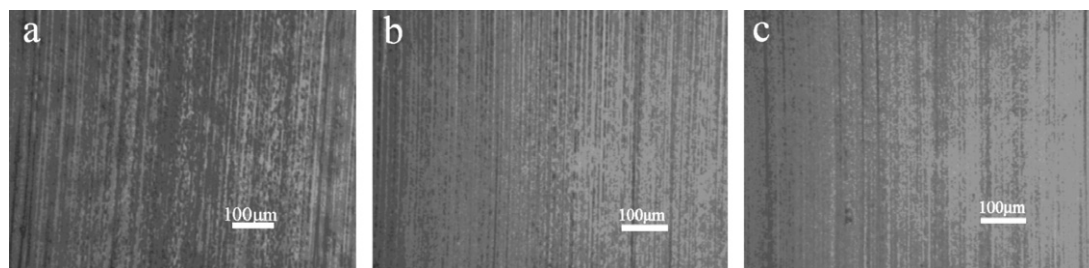


Fig. 12. Optical micrographs (OM) of the transfer films formed on the counterpart ring surface for the unfilled and filled PU coating (520 N, 2.56 m/s, and 60 min): (a) the unfilled; (b) with 1.0 wt.% of TiNTs; (c) with 1.0 wt.% of TiNTs–HDI.

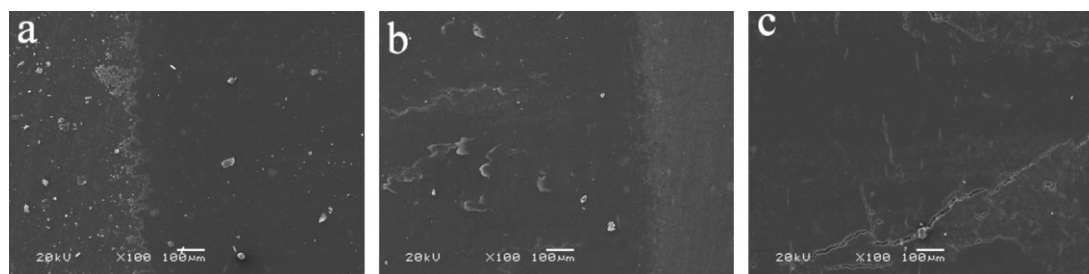


Fig. 13. SEM pictures of the worn surfaces of the PU coating reinforced with 1.0 wt.% TiNTs–HDI under different applied load (60 min): (a) 520 N; (b) 1120 N; (c) 1620 N.

of applied load on the worn surface. The worn surfaces of the 1.0 wt.% TiNTs filled PU coating are shown in Fig. 13a–c under different applied load. It can be seen that the worn surfaces of the filled PU coating are smooth at 2.56 m/s under 520 N (see Fig. 13a). When applied load is under 1120 N, there are some adhesion marks and cracks on the worn surfaces (see Fig. 13b). However, with further increase of applied load, the wear became from mild to severe, which can be seen from the comparison between Fig. 13b and c. The worn surface under 1620 N clearly shows large amounts of cracks (see Fig. 13c), which indicates that the serious fatigue wear is the main wear mechanism of the filled PU coating when sliding under higher applied load. It can be inferred that large area of frictional surface of the filled PU coating would flake away if the applied load increases further and the coating would be seriously damaged.

5. Conclusions

1. Grafting of HDI onto TiO₂ nanotubes increased the interfacial interaction between the nanotubes and the PU matrix through chemical bonding. It proved to be an effective way to further enhance the nano-effect of the nanotubes on the improvements of the tribological performance.
2. The dispersion of TiNTs in the PU coating is improved by modification with HDI, and the friction-reduction and anti-wear ability of TiNTs as lubricant additive are also improved by modification with HDI effectively.
3. The PU/TiNTs–HDI nanocomposite coating registers lower friction coefficient and higher wear life than the unfilled and TiNTs filled PU nanocomposite coating under dry sliding. TiNTs or TiNTs–HDI strengthen the structure of the PU coating and effectively reduce its adhesive and ploughing wear, and enhance the formation of the transfer films with better quality on the counterpart steel surface, which together with the load-carrying capacity of the TiNTs or TiNTs–HDI contributes to improve the friction-reduction and wear-resistance of the TiNTs or TiNTs–HDI filled PU composite coating.

References

- [1] Crawford DM, Escarsega JA. Dynamic mechanical analysis of novel polyurethane coating for military applications. *Thermochim Acta* 2000;357–358:161–8.
- [2] Bavykin DV, Friedrich JM, Walsh FC. Protonated titanates and TiO₂ nanostructured materials: synthesis, properties, and applications. *Adv Mater* 2006;18:2807–24.
- [3] Linsebigler AL, Lu GQ, Yates JT. Photocatalysis on TiO₂ surfaces: principles, mechanisms, and selected results. *Chem Rev* 1995;95:735.
- [4] Liaw WC, Chen KP. Preparation and characterization of poly(imide siloxane) (PIS)/titania(TiO₂) hybrid nanocomposites by sol–gel processes. *Eur Polym J* 2007;43(6):2265–78.
- [5] Amita V, Kar M, Agnihotry SA. Aging effect of diethanolamine stabilized sol on different properties of TiO₂ films: electrochromic applications. *Sol Energ Mat Sol C* 2007;91(14):1305–12.
- [6] Wang C, Deng ZX, Li Y. The synthesis of nanocrystalline anatase and rutile titania in mixed organic media. *Inorg Chem* 2001;40:5210.
- [7] Koenenkamp R, Henninger R, Hoyer P. Photocarrier transport in colloidal titanium dioxide films. *J Phys Chem* 1993;97(28):7328–30.
- [8] Wang YQ, Hu GQ, Duan XF, Sun HL, Xue QK. Microstructure and formation mechanism of titanium dioxide nanotubes. *Chem Phys Lett* 2002;365:427–31.
- [9] Lakshmi BB, Patrissi CJ, Martin CR. Sol–gel template synthesis of semiconductor oxide micro- and nanostructures. *Chem Mater* 1997;9:2544.
- [10] Miao Z, Xu D, Ouyang J, Guo G, Zhao X, Tang Y. Electrochemically induced sol–gel preparation of single-crystalline TiO₂ nanowires. *Nano Lett* 2002;2:717.
- [11] Kasuga T, Hiramatsu M, Hoson A, Sekino T, Niihara K. Formation of titanium oxide nanotube. *Langmuir* 1998;14:3160–3.
- [12] Stuart BH. Surface plasticisation of poly(ether ether ketone) by chloroform. *Polym Test* 1997;16:49–57.
- [13] Delucchi M, Barbucci A, Cerisola G. Influence of thickness on mechanical properties and crack-bridging ability of coatings for concrete. *Prog Org Coat* 1998;33:76.
- [14] Merdas I, ThomINETTE F, Tcharkhtchi A, Verdu J. Factors governing water absorption by composite matrices. *Compos Sci Technol* 2002;62:487–92.
- [15] Holmberg K, Matthews A, Ronkainen H. Coatings tribology-contact mechanisms and surface design. *Tribol Int* 1998;31(1–3):107–20.
- [16] Bonfield W, Edwards BC, Markham AJ, White JR. Wear transfer films formed by carbon fibre reinforced epoxy resin sliding on stainless steel. *Wear* 1976;37:113–21.
- [17] Suh NP. The delamination theory of wear. *Wear* 1973;25:111–24.